

Crystal Structures and Substitution Reactions of *trans*(O,S)-[Ru(bpy)Cl(dmso-*S*)$_2$(OH$_2$)]$^+$ and Three Derivative Complexes, *trans*(L,S)-[Ru(bpy)Cl(dmso-*S*)$_2$(L)]$^+$ (bpy: 2,2′-Bipyridine, dmso: Dimethyl Sulfoxide, L = dmso-*O*, MeOH, or MeCN)

Mari Toyama,* Shinobu Iwamatsu, Ken-ichi Inoue, and Noriharu Nagao*

Department of Applied Chemistry, Meiji University, Kawasaki 214-8571

Received August 16, 2010; E-mail: nori@isc.meiji.ac.jp

The labile cationic aqua complexes, *trans*(O,S)-[Ru(bpy)Cl(dmso-*S*)$_2$(OH$_2$)]X (**1·X**; X$^-$ = PF$_6^-$ or OTf$^-$: CF$_3$SO$_3^-$) have been prepared by the treatment of *cis*(Cl),*cis*(S)-[Ru(bpy)Cl$_2$(dmso-*S*)$_2$] with Ag$^+$ in water at room temperature. When **1·X** is dissolved in DMSO, MeOH, or MeCN, the OH$_2$ ligand in **1**$^+$ is replaced with a solvent molecule (L) to yield *trans*(L,S)-[Ru(bpy)Cl(dmso-*S*)$_2$(L)]$^+$ (L = dmso-*O*, **2**$^+$; L = MeOH, **3**$^+$; and L = MeCN, **4**$^+$), respectively. Moreover, **2·(OTf)** is also obtained by the reaction of *cis*(Cl),*cis*(S)-[Ru(bpy)Cl$_2$(dmso-*S*)$_2$] with Ag(OTf) in DMSO on refluxing. The four kinds of crystal structures of *trans*(L,S)-[Ru(bpy)Cl(dmso-*S*)$_2$(L)]PF$_6$ (**1·PF$_6$·H$_2$O**, **2·PF$_6$**, **3·PF$_6$**, and **4·PF$_6$·MeCN**) revealed that the structural parameters, except for the sixth axial ligand, were essentially the same, and the four ligands, the bpy, two dmso-*S*, and the equatorial Cl$^-$ ligands are connected by hydrogen bonding. All the OH$_2$, dmso-*O*, MeOH, or MeCN ligands on the sixth coordination site at the axial position in cationic mono(bpy)ruthenium(II) complexes are labile so they are interconvertable. The [Ru(bpy)Cl(dmso-*S*)$_2$] unit does not change at room temperature even in solutions due to the presence of hydrogen networks among the bpy, two dmso-*S*, and the equatorial Cl$^-$ ligands.

Ruthenium(II) polypyridyl complexes have been the subject of much interest due to their photochemical, electrochemical, and biochemical properties.[1–10] An important synthetic aspect of aqua complexes is their interconversion with hydroxo and oxo species via deprotonation or oxidation. There are a lot of reports on the ability of Ru–aqua polypyridyl complexes to lose protons and electrons and easily reach higher oxidation states.[11–20] On the other hand, Ru–aqua polypyridyl complexes have been recognized as versatile precursors for various complexes, because the aqua ligand in the complexes is usually so labile as to be replaced with other donor ligands.[21,22] They also are important as components of supramolecules. Moreover, recently ruthenium(II)- and ruthenium(III) compounds are the subjects of promising anticancer drug candidates.[23,24]

Most of the ruthenium polypyridine complexes that have hitherto been studied contain 2,2′-bipyridine (bpy) or analogous ligands. Previously, we have reported a convenient syntheses, isomerization reactions, and the crystal structures of [Ru(bpy)Cl$_2$(dmso-*S*)$_2$], *trans*(Cl),*cis*(S)-, *cis*(Cl),*cis*(S)-, and *cis*(Cl),*trans*(S)-isomers.[25] The *trans*(Cl),*cis*(S)-isomer is synthesized by the reaction of *trans*(Cl)-[RuCl$_2$(dmso-*S*)$_4$] with bpy in EtOH–H$_2$O at 273 K. The *cis*(Cl),*cis*(S)-isomer is prepared in EtOH–DMSO (9:1) by the reaction of *cis*(Cl),*fac*(S)-[RuCl$_2$(dmso-*O*)(dmso-*S*)$_3$] with bpy or by the isomerization of the *trans*(Cl),*cis*(S)-isomer. The thermodynamic stability of *cis*(Cl),*cis*(S)-isomer is greater than those of *trans*(Cl),*cis*(S)- and *cis*(Cl),*trans*(S)-isomers. Furthermore, the intramolecular hydrogen bonding, such as CH···O or CH···Cl–Ru interaction, between the bpy and dmso or Cl$^-$ ligands or between two dmso ligands, may explain the distortion, stability, and spectral features of mono(bpy)ruthenium(II) complexes [Ru(bpy)Cl$_2$-(dmso-*S*)$_2$].

In this paper, the *cis*(Cl),*cis*(S)-isomer was used as the synthetic precursor because of the greater thermodynamic stability of *cis*(Cl),*cis*(S)-isomer over other isomers. We will report the synthesis of *trans*(O,S)-[Ru(bpy)Cl(dmso-*S*)$_2$-(OH$_2$)]X (**1·X**; X$^-$ = PF$_6^-$ or OTf$^-$: CF$_3$SO$_3^-$) from *cis*(Cl),*cis*(S)-[Ru(bpy)Cl$_2$(dmso-*S*)$_2$]. Further, three complexes *trans*(L,S)-[Ru(bpy)Cl(dmso-*S*)$_2$(L)]$^+$ (L = dmso-*O*, **2**$^+$; L = MeOH, **3**$^+$; and L = MeCN, **4**$^+$) were derived from **1**$^+$. From the point of view of utilization as synthetic precursor, the substitution reaction of four cationic mono(bpy)ruthenium(II) complexes **1**$^+$, **2**$^+$, **3**$^+$, and **4**$^+$ were investigated by ^{1}H NMR spectroscopy. The crystal structures of **1·PF$_6$·H$_2$O**, **2·PF$_6$**, **3·PF$_6$**, and **4·PF$_6$·MeCN** are also reported.

Experimental

Ruthenium trichloride trihydrate was purchased from Furuya Kinzoku Co. All other solvents and chemicals were of reagent grade and were used without further purification. The precursor *cis*(Cl),*cis*(S)-[Ru(bpy)Cl$_2$(dmso-*S*)$_2$] was prepared as previously described.[25]

The ^{1}H NMR spectra (270 MHz) were recorded on a JEOL GSX-270 spectrometer. All spectra were recorded at room temperature unless otherwise noted, and as internal standards TMS (for DMSO-d_6, CD$_3$CN, and CD$_3$OD solutions), and DMSO (2.71 ppm, for D$_2$O solution)[26] were used. The aromatic signals of ^{1}H NMR spectra for the complexes were assigned on the basis of the coupling constants and ^{1}H–^{1}H COSY experiments.[27]

Published on the web December 2, 2010; doi:10.1246/bcsj.20100224

Synthesis of *trans*(O,S)-[Ru(bpy)Cl(dmso-*S*)$_2$(OH$_2$)]PF$_6$·H$_2$O (1·PF$_6$·H$_2$O). A suspension of orange solid *cis*(Cl),*cis*(S)-[Ru(bpy)Cl$_2$(dmso-*S*)$_2$] (0.50 g, 1.1 mmol) in H_2O (25 mL) was stirred at room temperature for 15 min, during which the suspension became homogeneous. Five milliliters of aqueous Ag(OTf) (0.28 g, 1.1 mmol) was added, and the reaction mixture was stirred for 5 min. The resulting AgCl was filtered off. The filtrate is a solution of *trans*(O,S)-[Ru(bpy)Cl(dmso-*S*)$_2$(OH$_2$)](OTf) (**1·(OTf)**). To the filtrate, NH_4PF_6 (0.28 g) was added to precipitate a yellow solid (**1·PF$_6$·H$_2$O**). The yellow precipitate was collected by filtration, washed with a small amount of cold water, and dried in vacuo (0.51 g, 75%). Yellow crystals suitable for X-ray crystallography were grown over several days from the aqueous solution of **1·PF$_6$·H$_2$O** at 275 K. Anal. Calcd for $RuF_6ClC_{14}N_2O_4PS_2H_{24}$: C, 26.69; H, 3.84; N, 4.44%. Found: C, 26.55; H, 3.84; N, 4.41%. ^{1}H NMR (270 MHz, D_2O): δ 9.67 (1H, d, $J = 6.0$ Hz, H-6′), 9.65 (1H, d, $J = 5.9$ Hz, H-6), 8.54 (1H, d, $J = 7.8$ Hz, H-3), 8.51 (1H, d, $J = 7.8$ Hz, H-3′), 8.30 (1H, t, $J = 7.8$ Hz, H-4), 8.21 (1H, t, $J = 7.8$ Hz, H-4′), 7.84 (1H, dd, $J = 5.9$ and 7.4 Hz, H-5), 7.71 (1H, dd, $J = 6.0$ and 7.5 Hz, H-5′), 3.53 (3H, s, CH_3 of dmso), 3.34 (3H, s, CH_3 of dmso), 3.04 (3H, s, CH_3 of dmso), and 2.52 (3H, s, CH_3 of dmso).

Synthesis of *trans*(O,S)-[Ru(bpy)Cl(dmso-*O*)(dmso-*S*)$_2$]-PF$_6$ (2·PF$_6$). A solution of **1·PF$_6$** (0.21 g, 0.35 mmol) in DMSO (1 mL) was stirred at room temperature for 10 min to replace the OH_2 ligand in **1·PF$_6$** with a dmso molecule. Ethanol (2 mL) and diethyl ether (15 mL) were added to the solution to precipitate a yellow solid (**2·PF$_6$**). The yellow precipitate was washed several times by decantation with a small amount of diethyl ether, and was collected by filtration, washed with diethyl ether, and dried in vacuo (0.19 g, 80%). Yellow crystals of **2·PF$_6$** suitable for X-ray crystallography were obtained by vapor diffusion of diethyl ether into an EtOH–DMSO (1:1) solution of **2·PF$_6$**. Anal. Calcd for $RuF_6ClC_{16}N_2O_3PS_3H_{26}$: C, 28.59; H, 3.90; N, 4.17%. Found: C, 28.68; H, 3.91; N, 4.20%. ^{1}H NMR (270 MHz, DMSO-d_6): δ 9.73 (1H, d, $J = 5.7$ Hz, H-6′), 9.62 (1H, d, $J = 5.7$ Hz, H-6), 8.79 (1H, d, $J = 7.9$ Hz, H-3), 8.72 (1H, d, $J = 8.2$ Hz, H-3′), 8.41 (1H, t, $J = 7.8$ Hz, H-4), 8.23 (1H, t, $J = 7.8$ Hz, H-4′), 7.94 (1H, dd, $J = 5.8$ and 7.4 Hz, H-5), 7.73 (1H, dd, $J = 5.9$ and 7.5 Hz, H-5′), 3.46 (3H, s, CH_3 of dmso), 3.15 (3H, s, CH_3 of dmso), 3.01 (3H, s, CH_3 of dmso), 2.62 (3H, s, CH_3 of dmso), 2.43 (3H, s, CH_3 of dmso), and 2.01 (3H, s, CH_3 of dmso).

Synthesis of *trans*(O,S)-[Ru(bpy)Cl(dmso-*O*)(dmso-*S*)$_2$]-(OTf) (2·(OTf)). Method A: The procedure was similar to that of **2·PF$_6$**. In this case, **1·(OTf)** was used instead of **1·PF$_6$**. Water was stripped off from the aqueous solution of **1·(OTf)** with an evaporator. The residue (yellow oil) was treated with DMSO, EtOH, and diethyl ether successively, to form a yellow solid (**2·(OTf)**), which was collected by filtration, washed with diethyl ether, and dried in vacuo (80%). Anal. Calcd for $RuF_3ClC_{17}N_2O_6S_4H_{26}$: C, 30.19; H, 3.87; N, 4.14%. Found: C, 30.03; H, 3.82; N, 4.09%.

Method B: A suspension of *cis*(Cl),*cis*(S)-[Ru(bpy)Cl$_2$-(dmso-*S*)$_2$] (1.0 g, 2.1 mmol) in DMSO (5 mL) was refluxed under Ar atmosphere for 30 min, during which the suspension became homogeneous. Equimolar Ag(OTf) (0.53 g, 2.1 mmol) was added, and the reaction mixture was heated for 5 min. The resulting AgCl precipitate was removed by filtration. After the filtrate was cooled to room temperature, EtOH (20 mL) and diethyl ether (80 mL) were added to precipitate a yellow solid (**2·(OTf)**). The precipitate was washed several times by decantation with a small amount of diethyl ether, and was collected by filtration, washed with diethyl ether, and dried in vacuo (1.3 g, 92%).

Synthesis of *trans*(O,S)-[Ru(bpy)Cl(dmso-*S*)$_2$(MeOH)]-PF$_6$ (3·PF$_6$). A suspension of orange solid **1·PF$_6$** (0.20 g, 0.33 mmol) in MeOH (5 mL) was stirred at room temperature for 5 min. While stirring, the suspension became homogeneous (2 min), and then gradually yellow precipitate (**3·PF$_6$**) started to precipitate. To the reaction mixture, diethyl ether (25 mL) was added to complete the precipitation of **3·PF$_6$**. The precipitate was collected by filtration, washed with diethyl ether, and dried in vacuo (0.18 g, 80%). Yellow crystals of **3·PF$_6$** suitable for X-ray crystallography were obtained by vapor diffusion of diethyl ether in to a MeOH solution of **3·PF$_6$**. Anal. Calcd for $RuF_6ClC_{15}N_2O_3PS_2H_{24}$: C, 28.78; H, 3.86; N, 4.48%. Found: C, 28.74; H, 3.90; N, 4.47%. ^{1}H NMR (270 MHz, CD_3OD): δ 9.93 (1H, d, $J = 5.8$ Hz, H-6′), 9.77 (1H, d, $J = 5.7$ Hz, H-6), 8.69 (1H, d, $J = 8.1$ Hz, H-3), 8.64 (1H, d, $J = 8.3$ Hz, H-3′), 8.35 (1H, t, $J = 7.9$ Hz, H-4), 8.25 (1H, t, $J = 7.8$ Hz, H-4′), 7.87 (1H, dd, $J = 5.7$ and 7.6 Hz, H-5), 7.73 (1H, dd, $J = 5.9$ and 7.5 Hz, H-5′), 3.58 (3H, s, CH_3 of dmso), 3.34 (3H, s, CH_3 of MeOH), 3.28 (3H, s, CH_3 of dmso), 3.11 (3H, s, CH_3 of dmso), and 2.33 (3H, s, CH_3 of dmso).

Synthesis of *trans*(O,S)-[Ru(bpy)Cl(dmso-*S*)$_2$(MeOH)]-(OTf) (3·(OTf)). This was prepared in a similar manner to **2·(OTf)** (Method A) by using MeOH in place of DMSO. The yellow oil residue **1·(OTf)** (0.6 mmol) was dissolved in MeOH (5 mL) to get the yellow solution, which was evaporated to dryness under vacuum. This treatment was repeated three times to complete the substitution of the OH_2 ligand with MeOH. Finally MeOH (3 mL) was added to the residue, and then diethyl ether (30 mL) was added to obtain a yellow solid (**3·(OTf)**). This was collected by filtration, washed with diethyl ether, and dried in vacuo (0.37 g, 93%). Anal. Calcd for $RuF_3ClC_{16}N_2O_6S_3H_{24}$: C, 30.50; H, 3.84; N, 4.45%. Found: C, 30.60; H, 4.02; N, 4.43%.

Synthesis of *trans*(N,S)-[Ru(bpy)Cl(dmso-*S*)$_2$(MeCN)]-PF$_6$·MeCN (4·PF$_6$·MeCN). This was prepared in a similar manner to **3·PF$_6$** by using MeCN in place of MeOH. The solid **1·PF$_6$** was treated with MeCN to form yellow precipitate (**4·PF$_6$**), which was collected by filtration, washed with diethyl ether, and dried in vacuo (0.19 g, 90%). Yellow crystals of **4·PF$_6$·MeCN** suitable for X-ray crystallography were obtained by vapor diffusion of diethyl ether into an acetonitrile solution of **4·PF$_6$**. Anal. Calcd for $RuF_6ClC_{16}N_3O_2PS_2H_{23}$: C, 30.26; H, 3.65; N, 6.62%. Found: C, 30.15; H, 3.64; N, 6.62%. ^{1}H NMR (270 MHz, CD_3CN): δ 9.83 (1H, d, $J = 5.8$ Hz, H-6′), 9.65 (1H, d, $J = 5.6$ Hz, H-6), 8.46 (1H, d, $J = 7.9$ Hz H-3), 8.42 (1H, d, $J = 7.9$ Hz, H-3′), 8.25 (1H, t, $J = 7.9$ Hz, H-4), 8.15 (1H, t, $J = 7.9$ Hz, H-4′), 7.80 (1H, dd, $J = 7.6$ and 5.7 Hz, H-5), 7.67 (1H, dd, $J = 5.7$ and 7.6 Hz, H-5′), 3.45 (3H, s, CH_3 of dmso), 3.35 (3H, s, CH_3 of dmso), 2.90 (3H, s, CH_3 of dmso),

Table 1. Crystallographic Data for **1·PF$_6$·H$_2$O**, **2·PF$_6$**, **3·PF$_6$**, and **4·PF$_6$·MeCN**

	1·PF$_6$·H$_2$O	**2·PF$_6$**	**3·PF$_6$**	**4·PF$_6$·MeCN**
Experimental formula	$Ru_1F_6Cl_1C_{14}N_2O_4P_1S_2H_{24}$	$Ru_1F_6Cl_1C_{16}N_2O_3P_1S_3H_{26}$	$Ru_1F_6Cl_1C_{15}N_2O_3P_1S_2H_{24}$	$Ru_1F_6Cl_1C_{18}N_4O_2P_1S_2H_{26}$
Formula weight	629.96	672.06	625.97	676.04
Crystal system	monoclinic	monoclinic	monoclinic	monoclinic
Space group	$P2_1/c$ (# 14)	$P2_1/c$ (# 14)	$P2_1/c$ (# 14)	$P2_1/c$ (# 14)
Lattice parameters				
a/Å	12.714(2)	10.141(2)	12.46(1)	10.314(2)
b/Å	12.850(2)	24.474(5)	12.77(1)	8.294(2)
c/Å	14.144(2)	10.464(2)	14.22(1)	31.117(7)
α/°	90	90	90	90
β/°	90.6288(5)	92.8408(2)	90.195(4)	91.4761(9)
γ/°	90	90	90	90
V/Å^3	2310.6(5)	2593.7(10)	2262.5(3)	2661(1)
Z	4	4	4	4
D_{calcd}/g cm^{-3}	1.811	1.721	1.838	1.687
F_{000}	1264.00	1352.00	1256.00	1360.00
μ (Mo Kα, cm^{-1})	11.16	10.75	11.36	9.72
Independent reflection	4701	4104	2424	4417
Data to parameter ratio	18.98	22.24	20.75	19.76
$R1$ [$I > 2\sigma(I)$]/ No. of reflection	0.035/4701	0.067/4104	0.062/2424	0.042/4417
$wR2$ (all data)	0.105/5313	0.198/6628	0.136/5810	0.120/6265
GOF	1.45	1.41	0.97	1.11

Table 2. Selected Bond Lengths (Å) for **1·PF$_6$·H$_2$O**, **2·PF$_6$**, **3·PF$_6$**, and **4·PF$_6$·MeCN**

	trans[a)]	**1·PF$_6$·H$_2$O**	**2·PF$_6$**	**3·PF$_6$**	**4·PF$_6$·MeCN**
Ru–N bond	Cl	Ru(1)–N(1) 2.081(2)	Ru(1)–N(1) 2.079(4)	Ru(1)–N(1) 2.068(6)	Ru(1)–N(1) 2.082(3)
	S	Ru(1)–N(2) 2.100(2)	Ru(1)–N(2) 2.077(5)	Ru(1)–N(2) 2.090(5)	Ru(1)–N(2) 2.105(3)
					Ru(1)–N(3) 2.091(3)
Ru–Cl bond	N	Ru(1)–Cl(1) 2.392(1)	Ru(1)–Cl(1) 2.399(2)	Ru(1)–Cl(1) 2.383(2)	Ru(1)–Cl(1) 2.390(1)
Ru–S bond	O	Ru(1)–S(1) 2.213(1)	Ru(1)–S(1) 2.209(2)	Ru(1)–S(1) 2.207(2)	
	N	Ru(1)–S(2) 2.287(1)	Ru(1)–S(2) 2.309(2)	Ru(1)–S(2) 2.274(2)	Ru(1)–S(2) 2.293(1)
					Ru(1)–S(1) 2.261(1)
Ru–O bond	S	Ru(1)–O(3) 2.137(2)	Ru(1)–O(3) 2.146(4)	Ru(1)–O(3) 2.155(5)	
S–O bond	O	S(1)–O(1) 1.487(2)	S(1)–O(1) 1.461(5)	S(1)–O(1) 1.477(5)	S(1)–O(1) 1.487(3)
		S(2)–O(2) 1.488(2)	S(2)–O(2) 1.482(6)	S(2)–O(2) 1.457(5)	S(2)–O(2) 1.488(3)
	S		S(3)–O(3) 1.529(5)		

a) Coordinated atom in *trans* position.

2.25 (3H, s, CH_3 of dmso), 2.05 (3H, s, CH_3 of MeCN), and 1.96 (3H, s, CH_3 of free MeCN).

Synthesis of *trans*(N,S)-[Ru(bpy)Cl(dmso-*S*)$_2$(MeCN)](OTf) (4·(OTf)). This procedure was similar to that for **3·(OTf)**, but using MeCN in place of MeOH. The solid **3·(OTf)** was treated with MeCN to get yellow product (**4·(OTf)**) (75%). Anal. Calcd for $RuF_3ClC_{17}N_3O_5S_3H_{23}$: C, 31.94; H, 3.63; N, 6.58%. Found: C, 31.54; H, 3.54; N, 6.50%.

X-ray Crystallography. Data for all crystals were collected on a Rigaku/MSC Mercury CCD diffractometer with graphite-monochromated Mo Kα radiation ($\lambda = 0.71070$ Å) at 293 K. All calculations were carried out on an O_2 workstation (SGI) using the teXsan crystallographic software package of Molecular Structure Corporation.[28] The structures were solved by the direct method and expanded using Fourier techniques. The non-hydrogen atoms were refined anisotropically. Hydrogen atoms were positioned in idealized positions and included in the structure factor calculations. For **1·PF$_6$**, one H_2O molecule was included at a general position. For **4·PF$_6$**, one MeCN molecule was included at a general position. The crystallographic data, selected bond lengths and bond angles are listed in Tables 1, 2, and 3, respectively.

Crystallographic data have been deposited with Cambridge Crystallographic Data Centre: Deposition numbers CCDC-793712–793715 for compounds **1·PF$_6$·H$_2$O**, **2·PF$_6$**, **3·PF$_6$**, and **4·PF$_6$·MeCN**, respectively. Copies of the data can be obtained free of charge via http://www.ccdc.cam.ac.uk/conts/retrieving.html (or from the Cambridge Crystallographic Data Centre, 12, Union Road, Cambridge, CB2 1EZ, U.K.; fax: +44 1223 336033; e-mail: deposit@ccdc.cam.ac.uk).

Results and Discussion

Synthesis and Characterization of 1·PF$_6$. The synthetic route of **1·X** ($X^- = PF_6^-$ and OTf^-) is shown in Scheme 1. When dissolved in water, *cis*(Cl),*cis*(S)-[Ru(bpy)Cl$_2$(dmso-*S*)$_2$] immediately releases the axial Cl^- anion to give the cationic

Table 3. Selected Bond Angles (°) for **1·PF$_6$·H$_2$O**, **2·PF$_6$**, **3·PF$_6$**, and **4·PF$_6$·MeCN**

1·PF$_6$·H$_2$O		**2·PF$_6$**		**3·PF$_6$**		**4·PF$_6$·MeCN**	
Axial							
S(1)–Ru(1)–O(3)	175.65(6)	S(1)–Ru(1)–O(3)	174.5(1)	S(1)–Ru(1)–O(3)	175.3(1)	S(1)–Ru(1)–N(3)	177.35(10)
Axial–Equatorial							
S(1)–Ru(1)–N(1)	90.90(7)	S(1)–Ru(1)–N(1)	90.3(1)	S(1)–Ru(1)–N(1)	90.3(2)	S(1)–Ru(1)–N(1)	93.45(9)
S(1)–Ru(1)–N(2)	91.25(6)	S(1)–Ru(1)–N(2)	94.0(1)	S(1)–Ru(1)–N(2)	92.4(2)	S(1)–Ru(1)–N(2)	92.80(9)
S(1)–Ru(1)–Cl(1)	92.04(3)	S(1)–Ru(1)–Cl(1)	95.91(7)	S(1)–Ru(1)–Cl(1)	91.67(8)	S(1)–Ru(1)–Cl(1)	91.04(4)
S(1)–Ru(1)–S(2)	95.84(3)	S(1)–Ru(1)–S(2)	92.75(7)	S(1)–Ru(1)–S(2)	95.14(8)	S(1)–Ru(1)–S(2)	88.68(4)
O(3)–Ru(1)–N(1)	89.49(9)	O(3)–Ru(1)–N(1)	84.2(2)	O(3)–Ru(1)–N(1)	92.0(2)	N(3)–Ru(1)–N(1)	89.0(1)
O(3)–Ru(1)–N(2)	84.58(9)	O(3)–Ru(1)–N(2)	84.1(2)	O(3)–Ru(1)–N(2)	84.0(2)	N(3)–Ru(1)–N(2)	86.8(1)
O(3)–Ru(1)–Cl(1)	87.00(6)	O(3)–Ru(1)–Cl(1)	89.4(1)	O(3)–Ru(1)–Cl(1)	85.5(1)	N(3)–Ru(1)–Cl(1)	86.37(10)
O(3)–Ru(1)–S(2)	88.42(6)	O(3)–Ru(1)–S(2)	89.0(2)	O(3)–Ru(1)–S(2)	88.6(1)	N(3)–Ru(1)–S(2)	91.89(9)
Equatorial							
N(1)–Ru(1)–N(2)	78.31(9)	N(1)–Ru(1)–N(2)	79.9(2)	N(1)–Ru(1)–N(2)	78.9(2)	N(1)–Ru(1)–N(2)	78.1(1)
Cl(1)–Ru(1)–S(2)	90.68(3)	Cl(1)–Ru(1)–S(1)	95.91(7)	Cl(1)–Ru(1)–S(1)	91.67(8)	Cl(1)–Ru(1)–S(1)	91.04(4)
S(2)–Ru(1)–N(1)	96.78(6)	S(2)–Ru(1)–N(1)	98.5(1)	S(2)–Ru(1)–N(1)	97.1(2)	S(2)–Ru(1)–N(1)	93.45(9)
Cl(1)–Ru(1)–N(2)	93.83(6)	Cl(1)–Ru(1)–N(2)	92.8(1)	Cl(1)–Ru(1)–N(2)	93.3(2)	Cl(1)–Ru(1)–N(2)	92.72(10)
Dihedral angle							
Plane(1)–Plane(2)[a]	8.4(1)	Plane(1)–Plane(2)[a]	10.4(2)	Plane(1)–Plane(2)[a]	8.2(3)	Plane(1)–Plane(2)[a]	4.5(2)

a) Plane(1): N(1), C(1), C(2), C(3), C(4), C(5), Plane(2): N(2), C(6), C(7), C(8), C(9), C(10).

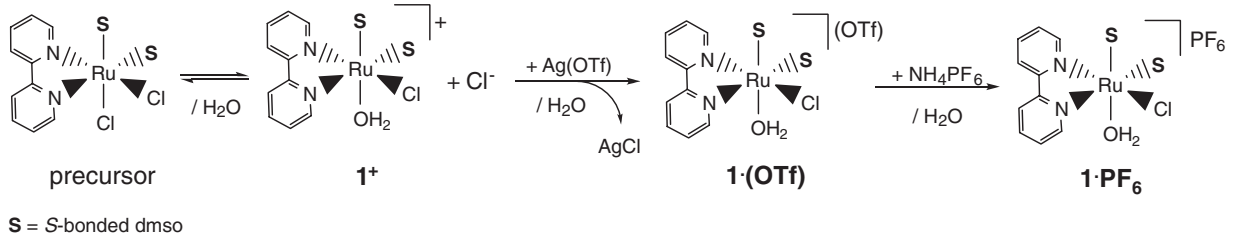

Scheme 1.

complex **1**$^+$. After stirring *cis*(Cl),*cis*(S)-[Ru(bpy)Cl$_2$(dmso-*S*)$_2$] in aqueous solution at room temperature, the same equivalent of Ag(OTf) was added and AgCl precipitated quantitatively (95%). After removal of the precipitate by filtration, the aqueous solution of **1·(OTf)** was obtained. To the aqueous solution of **1·(OTf)**, NH_4PF_6 was added to isolate as the yellow solid, **1·PF$_6$**. When water was removed from the aqueous solution of **1·(OTf)** by evaporation, no precipitation formed but yellow oil remained.

As shown in Figure 1, the ^{1}H NMR spectrum of **1·PF$_6$** in D_2O had one multiplet signal with intensities of 2H in the lowest field and six signals with an intensity of 1H in the aromatic region, and four signals with intensities of 3H in the aliphatic region. It was deduced from the signal intensities that **1**$^+$ had one bpy and two dmso ligands, and only a Cl^- ligand was replaced with an OH_2 ligand to give **1**$^+$. The ^{1}H NMR spectrum of **1·(OTf)** in D_2O was the same as that of **1·PF$_6$**. It showed that counter anions, PF_6^- and OTf^-, had no interaction with the cation **1**$^+$ in D_2O.

The crystal structure of **1·PF$_6$·H$_2$O** showed that the asymmetric unit contained one complex cation **1**$^+$, one counter-anion PF_6^-, and one H_2O molecule. An ORTEP drawing of the cation **1**$^+$ is shown in Figure 2. The Ru ion had a distorted octahedral geometry with the O atom of an OH_2 ligand *trans* to the S atom of a dmso ligand and *cis* to the S atom of another dmso ligand and a Cl atom (*cis*(Cl,S),*trans*(O,S)-geometry). The details of the structural parameters of **1**$^+$ are described later with **2**$^+$ in **2·PF$_6$**, **3**$^+$ in **3·PF$_6$**, and **4**$^+$ in **4·PF$_6$·MeCN**.

When **1**$^+$ was dissolved in various solvents, a solvent molecule readily replaced the OH_2 ligand. The rapid substitution reaction makes the syntheses of these complexes, **2**$^+$, **3**$^+$, and **4**$^+$, possible.

Substitution Reactions at Room Temperature. As shown in Scheme 2, these four cationic mono(bpy)ruthenium(II) complexes, **1**$^+$, **2**$^+$, **3**$^+$, and **4**$^+$, readily convert to each other. These substitution reactions were investigated by means of ^{1}H NMR spectroscopy. When **1**$^+$ was dissolved in CD_3OD at room temperature, the spectrum of the solution was the same as that of **3**$^+$ except for the signal of MeOH ligand and the signals of **1**$^+$ were not observed. These spectra revealed that an OH_2 ligand in **1**$^+$ was selectively exchanged with a CD_3OD

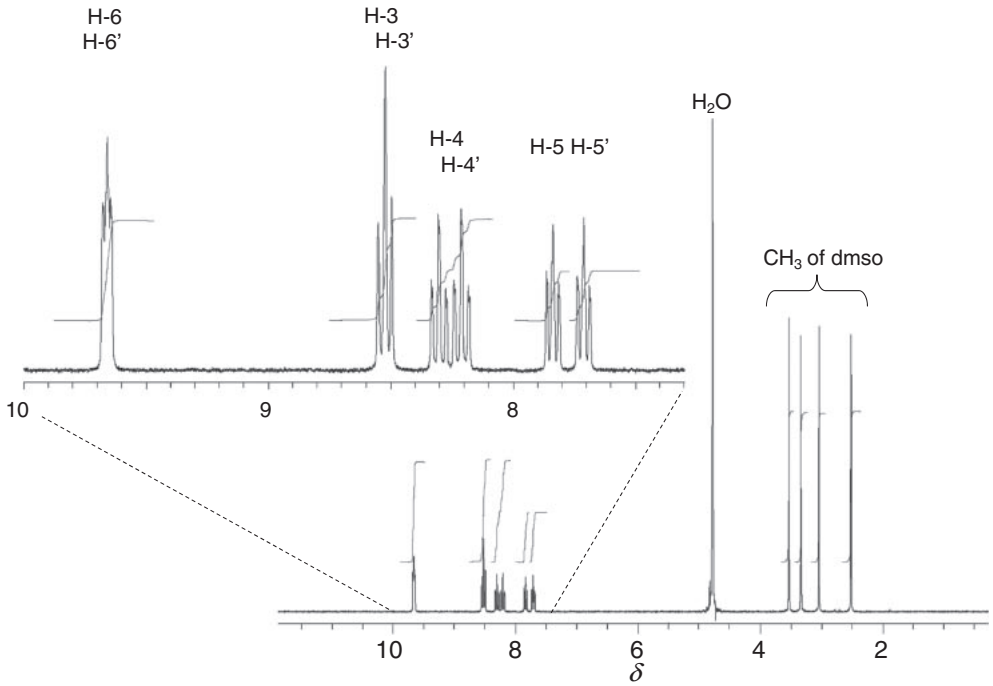

Figure 1. ^{1}H NMR spectrum of *trans*(O,S)-[Ru(bpy)Cl(dmso-*S*)$_2$(OH$_2$)]PF$_6$·H$_2$O (**1·PF$_6$·H$_2$O**) in D$_2$O.

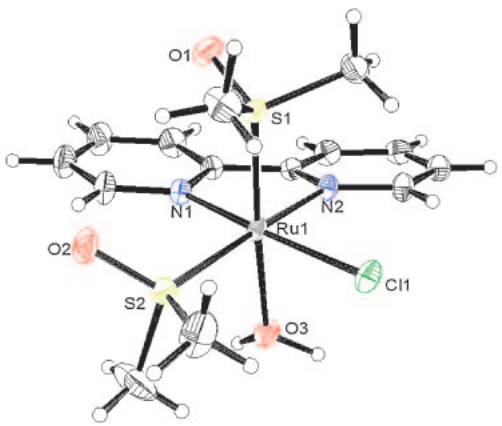

Figure 2. ORTEP drawing of the cation of **1·PF$_6$·H$_2$O** with 30% probability ellipsoids. The PF_6^- anion and an H_2O molecule are omitted for clarity.

molecule to form *trans*(O,S)-[Ru(bpy)(CD$_3$OD)Cl(dmso-*S*)$_2$]$^+$, **3**$_{CD_3OD}^+$ and this substitution reaction proceeded quickly. Such substitution reaction of **1**$^+$ was also observed in other solvents, DMSO-d_6 and CD$_3$CN (Scheme 2). Moreover, other complexes, **2**$^+$, **3**$^+$, and **4**$^+$, have also an analogs substitution reaction.

When **2**$^+$ or **3**$^+$ was dissolved in D$_2$O at room temperature, a dmso-*O* or a MeOH ligand was completely released to form *trans*(O,S)-[Ru(bpy)Cl(dmso-*S*)$_2$(OD$_2$)]$^+$, **1**$_{OD_2}^+$. When **4**$^+$ was dissolved in D$_2$O, a signal with an intensity of 3H due to the coordinate MeCN remained for a while, during which a signal due to free MeCN came out. When the solution was kept for one day at room temperature, signals due to **4**$^+$ completely disappeared and only signals due to **1**$_{OD_2}^+$ were observed. The reaction of **4**$^+$ in other solvents DMSO-d_6 or CD$_3$OD was similar to that in D$_2$O. The ligand L at the sixth coordination

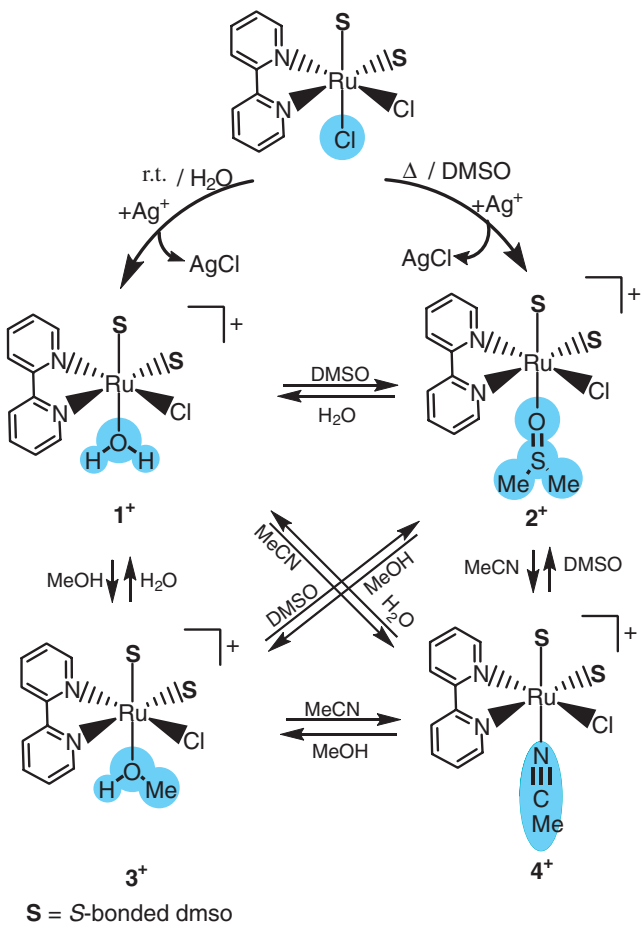

Scheme 2.

site in *trans*(O,S)-[Ru(bpy)Cl(dmso-*S*)$_2$(L)]$^+$ (L = OH_2, dmso-*O*, or MeOH) was labile, without depending on the kinds of solvent and L. However, substitution of the MeCN ligand in **4**$^+$ was less labile. Such selective exchange reactions of **1**$^+$, **2**$^+$, **3**$^+$, and **4**$^+$ showed that only the sixth coordination site was labile, other monodentate ligands a Cl^- and two dmso-*S* ligands were not substituted, and the [Ru(bpy)Cl(dmso-*S*)$_2$]$^+$ unit was stable in the solution at room temperature.

The aqua complex **1·X** (X^- = PF_6^- and OTf^-) was easily converted to other cationic complexes **2·X**, **3·X**, and **4·X** (Scheme 2). The complex **2**$^+$ was synthesized in good yield by the treatment of *cis*(Cl),*cis*(S)-[Ru(bpy)Cl_2(dmso-*S*)$_2$] with Ag^+ on refluxing in DMSO solution (Method B). This reaction was similar to that in the corresponding mono(Hdpa)ruthenium(II) complex, *trans*(O,S)-[RuCl(dmso-*O*)(dmso-*S*)$_2$(Hdpa)](OTf) (Hdpa: di-2-pyridylamine).[29] The complexes **3**$^+$ and **4**$^+$ were not obtained directly from *cis*(Cl),*cis*(S)-[Ru(bpy)Cl_2(dmso-*S*)$_2$], due to its poor solubility in MeOH and MeCN. The OH_2 ligand in **1**$^+$ was stripped off with solvent MeOH to afford **3**$^+$ in high purity. When **3**$^+$ was treated with MeCN, MeOH was easily removed to afford **4**$^+$ in high purity.

For each complex, PF_6^- salts are more suitable to get crystals for X-ray analysis. The OTf^- salts are more convenient as precursors for syntheses of other complexes due to their high solubility in various solvents.

The ^{1}H NMR spectra of **2·PF$_6$**, **3·PF$_6$**, and **4·PF$_6$·MeCN**, which are shown in Figures S1, S2, and S3, respectively, were the same as those of corresponding **2·(OTf)**, **3·(OTf)**, and **4·(OTf)**. It was revealed that counter anions, OTf^- and PF_6^-, had no interaction with the ruthenium complex cations in solution. The aromatic signals were assigned on the basis of the coupling constants[27] and ^{1}H–^{1}H COSY experiments. The methyl signals of dmso ligands were assigned by referring the spectra of the precursor *cis*(Cl),*cis*(S)-[Ru(bpy)Cl_2(dmso-*S*)$_2$][25] and the analogs mono(Hdpa)ruthenium(II) complex *trans*(O,S)-[RuCl(dmso-*O*)(dmso-*S*)$_2$(Hdpa)]$^+$.[29]

When **1**$^+$, **3**$^+$, and **4**$^+$ was dissolved in D_2O, CD_3OD, or CD_3CN, respectively, a coordinate L ligand, OH_2, MeOH, and MeCN, was replaced with the respective deuterated solvent molecules. On the other hand, the signals in the aromatic region did not change at room temperature for a few days. This suggests that the [Ru(bpy)Cl(dmso-*S*)$_2$]$^+$ unit in **1**$^+$, **3**$^+$, and **4**$^+$ was stable at room temperature.

When **2**$^+$ was dissolved in DMSO-d_6, both axial dmso ligands, L = dmso-*O* and dmso-*S*, are labile and have the same exchange rate in spite of their different coordination modes (*S*- and *O*-bonded) although the equatorial dmso ligand is inert. This observation suggests that mutual alternation of coordination mode of axial dmso ligands occurs, which is similar to that of the analogs mono(Hdpa)ruthenium(II) complex *trans*(O,S)-[RuCl(Hdpa)(dmso-*O*)(dmso-*S*)$_2$]$^+$.[29]

Substitution Reactions at 323 K. When D_2O solution of **1**$^+$ was heated for 3 h at 323 K, additional signals appeared (Figure S4). A signal at 2.71 ppm was assigned to free DMSO. It reveals that one or two dmso-*S* ligands were released from the complex cation. Similarly, when **3**$^+$ or **4**$^+$ was heated in the CD_3OD or CD_3CN solution, dmso-*S* ligands released from the complex cation (Figures S5 and S6, respectively). Furthermore, when Ag(OTf) was added to the heated aqueous **1**$^+$, AgCl precipitated. This showed that the equatorial Cl^- ligand also was released from the complex ion.

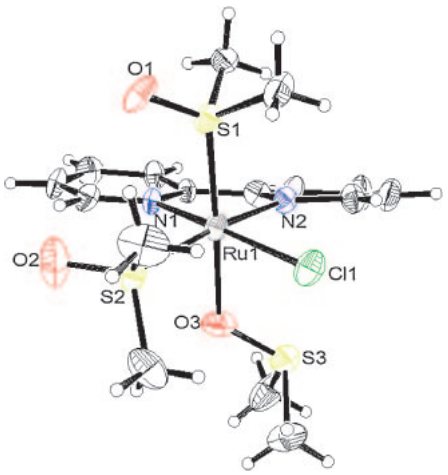

Figure 3. ORTEP drawing of the cation of **2·PF$_6$** with 30% probability ellipsoids. The PF_6^- anion is omitted for clarity.

When **2**$^+$ was heated in DMSO-d_6 solution at 323 K, the signals of dmso ligands disappeared and a signal of free DMSO appeared, which showed the exchange reaction of free DMSO-d_6 and coordinated dmso ligands occurred to form *trans*(O,S)-[Ru(bpy)Cl(dmso-d_6-*O*)(dmso-d_6-*S*)$_2$]$^+$. The chemical shift of signals for bpy ligand did not change. It showed that the equatorial Cl^- ligand did not leave or change its coordinate site in DMSO. This phenomenon demonstrates that the synthesis of **2**$^+$ by the reaction of *cis*(Cl),*cis*(S)-[Ru(bpy)Cl_2(dmso-*S*)$_2$] with Ag(OTf) in DMSO (Method B) is feasible.

We have previously reported the isomerization reaction of the precursor *cis*(Cl),*cis*(S)-[Ru(bpy)Cl_2(dmso-*S*)$_2$] in DMSO. The ^{1}H NMR spectrum of the solution after 1 h of heating at 363 K had extra signals of *cis*(Cl),*trans*(S)-isomer and an uncharacterized species in addition to the signals of *cis*(Cl),*cis*(S)-isomer (Figure 7 in Ref. 25). The signals of **2**$^+$ in this paper are identical with the signals of the uncharacterized species. Therefore, it is indicated that the precursor *cis*(Cl),*cis*(S)-[Ru(bpy)Cl_2(dmso-*S*)$_2$] in DMSO isomerizes to *cis*(Cl),*trans*(S)-isomer with an additional substitution reaction of the axial Cl^- ligand with a solvent DMSO molecule.

Crystal Structures. ORTEP drawings of three cations in **2·PF$_6$**, **3·PF$_6$**, and **4·PF$_6$·MeCN** are shown in Figures 3–5. These cations were similar to **1**$^+$, except for the axial monodentate ligand dmso-*O*, MeOH, or MeCN. In **2**$^+$, the third dmso ligand had *O*-bonded coordination. It may be due to the electronic effect by the *trans* dmso-*S* ligand and the steric interaction between the axial dmso-*S* and other ligands, similar to the case of the analogous mono(Hdpa)ruthenium(II) complex, *trans*(O,S)-[RuCl(dmso-*O*)(dmso-*S*)$_2$(Hdpa)]$^+$.[29]

Previously, the crystal structure of the precursor *cis*(Cl),*cis*(S)-[Ru(bpy)Cl_2(dmso-*S*)$_2$], revealed that there are attractive intramolecular hydrogen-bonding interactions (CH···O or CH···Cl) between the bpy and dmso or Cl^- ligands within the equatorial plane, and between the equatorial dmso and the axial dmso ligands.[25] Similar intracation hydrogen-bonding interactions within the equatorial plane were also

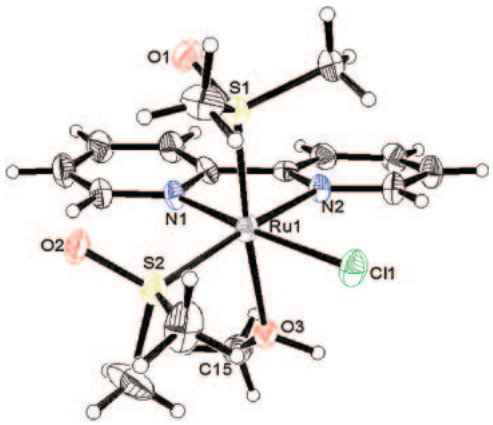

Figure 4. ORTEP drawing of the cation of **3·PF$_6$** with 30% probability ellipsoids. The PF_6^- anion is omitted for clarity.

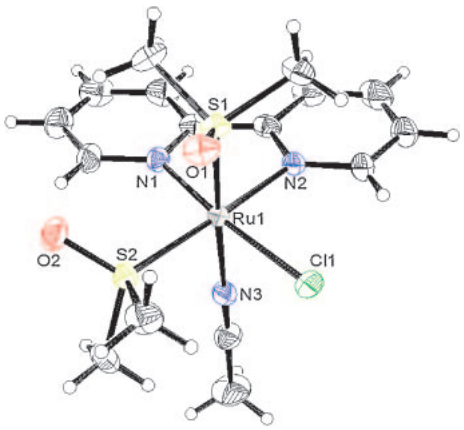

Figure 5. ORTEP drawing of the cation of **4·PF$_6$·MeCN** with 30% probability ellipsoids. The PF_6^- anion and an acetonitrile molecule are omitted for clarity.

observed in all four cationic mono(bpy)ruthenium(II) complexes **1**$^+$, **2**$^+$, **3**$^+$, and **4**$^+$ (Figures S7, S8, S9, and S10, respectively). The structural parameters and the conformations of dmso-*S*, Cl^-, and bpy ligands within the equatorial plane in these four cationic complexes, except for the axial ligands (L and dmso-*S*), were the essentially the same.

For cationic mono(bpy) complexes studied here, the Ru(1)–Cl(1) distances are similar (2.383(2)–2.399(2) Å). These are similar to the corresponding distances in *trans*(O,S)-[RuCl(dmso-*O*)(dmso-*S*)$_2$(Hdpa)](OTf) (2.399(1) and 2.398(1) Å).[29]

The Ru(1)–S(1) distances *trans* to an O atom of L in **1**$^+$, **2**$^+$, and **3**$^+$ (2.207(2)–2.213(1) Å) are similar to the corresponding distances in *trans*(O,S)-[RuCl(dmso-*O*)(dmso-*S*)$_2$(Hdpa)](OTf) (2.213(1) and 2.218(2) Å).[29] There is no difference in *trans* influence between three kinds of *O*-donor atoms in the OH_2, dmso-*O*, and MeOH ligands. For **4**$^+$, the Ru(1)–S(1) distance *trans* to the N atom of MeCN (2.261(1) Å) is slightly longer than the Ru(1)–S(1) distances of others. It is attributed to the greater *trans* influence of the acetonitrile ligand relative to the *O*-donor ligands.

The Ru(1)–S(2) distances *trans* to the pyridyl-N(2) rings in all four complexes (**1**$^+$, **2**$^+$, **3**$^+$, and **4**$^+$; 2.274(2)–2.309(2) Å) are longer than the Ru(1)–S(1) distance *trans* to the N atom of acetonitrile ligand (2.261(1) Å) in **4**$^+$, and similar to the corresponding in *trans*(O,S)-[RuCl(dmso-*O*)(dmso-*S*)$_2$(Hdpa)](OTf) (2.299(1) and 2.296(1) Å).[29] It may be due to the steric hindrance within the equatorial plane, composed of bpy, dmso-*S*, and Cl^- ligands.

Generally, an OH_2 and a dmso-*O* ligand are labile. In **1**$^+$, the Ru–O_{OH_2} distance (Ru(1)–O(3), 2.137(2) Å) is similar to those in previously reported Ru^{II}–OH_2 complexes (2.126(4)–2.152(4) Å).[11c,13,19,20] In **2**$^+$, the Ru–$O_{dmso\text{-}O}$ distance (Ru(1)–O(3), 2.146(4) Å) is comparable with those of *cis*(Cl),*fac*(S)-[$RuCl_2$(dmso-*O*)(dmso-*S*)$_3$] (2.134(3) Å)[24] and *cis*(Cl),*cis*(S),*cis*(O)-[$RuCl_2$(CO)(dmso-*S*)$_2$(dmso-*O*)] (2.123(2) Å),[30] in which the O atom are *trans* to the dmso-*S* ligands. The Ru–O distances in **1**$^+$ and **2**$^+$ support that the OH_2 ligand in **1**$^+$ and the dmso-*O* ligand in **2**$^+$ are also labile.

There are only a few reports on the crystal structures of Ru^{II}–MeOH complexes, *trans*-[Ru(dip)$_2$(MeOH)$_2$](OTf)$_2$ (dip: 4,7-diphenyl-1,10-phenanthroline; 2.090(4) Å)[31] (PPN)[Ru(dppe)(MeOH)(P_3O_9)] (PPN: $(Ph_3P)_2N^+$, $P_3O_9^{3-}$: *cyclo*-triphosphato, and dppe: $Ph_2PCH_2CH_2PPh_2$; 2.117 Å),[32] in which the MeOH is *trans* to the $P_3O_9^{3-}$ ligand, and [Ru(CH_2OMe)(CO)(MeOH)(terpy)]PF_6 (2.3127(17) Å),[33] in which the MeOH is *trans* to the CH_2OMe ligand.

For **4**$^+$, the Ru–N_{MeCN} distance (Ru(1)–N(3), 2.091(3) Å) is longer than that in [Ru(dmso-*S*)(MeCN)(phen-NH-phen)]-$(PF_6)_2$ (phen-NH-phen: *N*,*N*-bis(1,10-phenanthroline-2-yl)-amine); 2.064 Å),[34] in which the MeCN ligand is *trans* to the dmso-*S* ligand, and significantly longer than those of *cis*-[Ru(bpy)$_2$(MeCN)$_2$]$(PF_6)_2$ (2.033(7) and 2.033(6) Å),[35] *trans*-[Ru(bpy)$_2$(MeCN)$_2$]$(ClO_4)_2$ (2.008(4) Å),[36] [Ru(MeCN)(phen)(terpy)]$(PF_6)_2$ (2.041(5) Å),[37] [Ru(bpy)(MeCN)$_4$]$(PF_6)_2$ (*trans* to bpy, 2.043(2) and 2.047(2) Å; *trans* to MeCN, 2.027(2) and 2.025(2) Å),[38] and [RuCl(MeCN)$_5$]I·MeCN (*trans* to a Cl, 2.049(11) Å; *trans* to a MeCN, 2.003(10), 2.007(10), 2.013(10), and 2.024(10) Å).[39]

The conformation of the axial dmso-*S* ligand is dependent on the kind of the sixth axial ligand. In **2**$^+$ and **4**$^+$, in which the sixth axial ligands are without an OH group, the O atom of the axial dmso-*S* ligand is directed toward the methyl group of the equatorial dmso-*S* ligand (O(1)···H(19)C, 2.570 Å for **2**$^+$ and O(1)···H(17)C, 2.353 Å for **4**$^+$). The conformation of the axial dmso-*S* ligand is similar to that in the precursor *cis*(Cl),*cis*(S)-[Ru(bpy)Cl_2(dmso-*S*)$_2$], in which there are attractive intramolecular hydrogen-bonding interactions (CH···O or CH···Cl) between the bpy and dmso-*S* or Cl^- ligands within the equatorial plane, and between the equatorial dmso and the axial dmso ligands.[25] Therefore, in **2**$^+$ and **4**$^+$ four ligands, the bpy, two dmso-*S*, and the equatorial Cl^-, with intracation hydrogen bonding act as a pentadentate ligand, which coordinates to a Ru^{II} ion.

On the other hand, in **1**$^+$ and **3**$^+$, in which the sixth axial ligands L have an OH group, the O atom of the axial dmso ligand is directed toward the OH group of the axial ligand L of adjoining cation to form intercation hydrogen bonding. The crystal of **1·PF$_6$·H$_2$O** is composed of infinite chains of **1**$^+$ cations and H_2O molecules linked by three kinds of hydrogen bonds (Figure S11). The first hydrogen bond is observed between an H atom of the OH_2 ligand and an O(1) atom of

Table 4. Chemical Shifts of ^{1}H NMR Spectra of the Precursor *cis*(Cl),*cis*(S)-[Ru(bpy)Cl_2(dmso-*S*)$_2$],[25] $\mathbf{1}^+$, $\mathbf{2}^+$, $\mathbf{3}^+$, and $\mathbf{4}^+$

	cis(Cl),*cis*(S)-[Ru(bpy)Cl_2(dmso-*S*)$_2$] in DMSO-d_6[25]	$\mathbf{1}^+$ in D_2O	$\mathbf{2}^+$ in DMSO-d_6	$\mathbf{3}^+$ in CD_3OD	$\mathbf{4}^+$ in CD_3CN
H-6, H-6′	9.56, 9.66	9.65, 9.67	9.62, 9.73	9.77, 9.93	9.65, 9.83
$\Delta(\delta_{H\text{-}6} - \delta_{H\text{-}6'})$	(−0.10)	(−0.02)	(−0.11)	(−0.16)	(−0.18)
H-3, H-3′	8.65, 8.60	8.54, 8.51	8.79, 8.72	8.69, 8.64	8.46, 8.42
$\Delta(\delta_{H\text{-}3} - \delta_{H\text{-}3'})$	(0.05)	(0.03)	(0.07)	(0.05)	(0.04)
H-4, H-4′	8.21, 8.10	8.30, 8.21	8.41, 8.23	8.35, 8.25	8.25, 8.15
$\Delta(\delta_{H\text{-}4} - \delta_{H\text{-}4'})$	(0.11)	(0.09)	(0.18)	(0.10)	(0.10)
H-5, H-5′	7.77, 7.60	7.84, 7.71	7.94, 7.73	7.87, 7.73	7.80, 7.67
$\Delta(\delta_{H\text{-}5} - \delta_{H\text{-}5'})$	(0.17)	(0.13)	(0.21)	(0.14)	(0.13)
Equatorial dmso	3.40, 3.37	3.53, 3.34	3.46, 3.15	3.58, 3.28	3.45, 3.35
$\Delta\delta$	(0.03)	(0.19)	(0.31)	(0.30)	(0.10)
Axial dmso	2.98, 2.28	3.04, 2.52	3.01, 2.62, 2.43, 2.01	3.11, 2.33	2.90, 2.25
$\Delta\delta$	(0.70)	(0.52)		(0.78)	(0.65)
Free DMSO[26]	2.54	2.71	2.54	2.65	2.50

the dmso-S(1) ligand on the adjoining Ru(1) cation. The second one is between another H atom of the OH_2 ligand and an O(4) atom of an H_2O molecule, and the third one is between an H atom of an adjoining H_2O molecule and the O(2) atom of the dmso-S(2) ligand on the Ru(1) cation. The crystal of $\mathbf{3}\cdot\mathbf{PF_6}$ also is composed of infinite chains of $\mathbf{3}^+$ cations linked by two kinds of hydrogen bonds (Figure S12). The first hydrogen bond is between an H atom of the OH group of the MeOH ligand and an O(1) atom of the dmso-S(1) ligand on the adjoining Ru(1) cation. The second one is between an H atom of the methyl group of the MeOH ligand and the O(2) atom of the dmso-S(2) ligand on the adjoining Ru(1) cation.

^{1}H NMR Spectroscopy. The chemical shifts and assignment of ^{1}H NMR spectra of $\mathbf{1}^+$, $\mathbf{2}^+$, $\mathbf{3}^+$, $\mathbf{4}^+$, and the precursor *cis*(Cl),*cis*(S)-[Ru(bpy)Cl_2(dmso-*S*)$_2$] are summarized in Table 4. The assignment of the signals was performed on the basis of the coupling constants.[27] On the basis of ^{1}H–^{1}H COSY, the signals of the bpy ligand could be classified into two pyridine rings which have four signals coupled with each other (H-3–H-6 and H-3′–H-6′). For all complexes, the signals of the protons H-3′, H-4′, and H-5′ are shifted upfield with respect to the protons H-3, H-4, and H-5, respectively. On the other hand, the signals of the proton H-6′ are shifted downfield with respect to the proton H-6, only for $\mathbf{1}^+$ the difference between H-6 and H-6′, $\Delta(\delta_{H\text{-}6} - \delta_{H\text{-}6'}) = -0.02$, is smaller than those of $\mathbf{2}^+$ (−0.11), $\mathbf{3}^+$ (−0.16), $\mathbf{4}^+$ (−0.18), and the precursor (−0.10). These observations indicate the structures of the complexes in the solvents are similar.

In assigning the two groups of signals to the pyridine rings, we assumed that H-6′ proton belongs the pyridine ring cis to the equatorial dmso ligand or trans to the chloro ligand. The downfield sift of H-6′ proton is due to the intracation hydrogen-bonding interaction between the H-6′ proton and the O atom of the equatorial dmso ligand (CH···OS). The tentative assignment of the signals H-3′–H-6′ to the pyridine ring trans to the chloro ligand is supported by the upfield shifts of H-3′, H-4′, and H-5′. In a paper, we reported that for *trans*(Cl),*cis*(S)-[Ru(bpy)-Cl_2(dmso-*S*)$_2$] (δ H-3, 8.62; H-4, 8.15; H-5, 7.65; and H-6, 9.65 in DMSO-d_6), both the pyridine rings of bpy are trans to the dmso-*S* ligands and equivalent by the two rotating dmso ligands.[25] For *cis*(Cl),*trans*(S)-[Ru(bpy)Cl_2(dmso-*S*)$_2$] (δ H-3, 8.50; H-4, 8.07; H-5, 7.65; and H-6, 9.39 in DMSO-d_6), both of the pyridine rings of the bpy are equivalent and trans to the chloro ligands.[25] The signals for the protons of the pyridine ring trans to chloro ligand appear upfield of those for the corresponding protons of the pyridine ring trans to dmso-*S* ligand. The deshielding effect on the protons of the pyridine ring due to trans chloro ligand is weaker than that due to trans dmso-*S* ligand, suggesting that the upfield signals H-3′, H-4′, and H-5′ are assignable to the pyridine ring trans to the chloro ligand and the signal of H-6′ also should appear upfield. Therefore, the downfield shift of H-6′ indicates the additional deshielding effect on H-6′ due to through space interaction, i.e., hydrogen-bonding interaction between the H-6′ proton and the O atom of the equatorial dmso ligand (CH···OS), which is consistent with the tentative assignment. For $\mathbf{1}^+$, the small difference between H-6 and H-6′, $\Delta(\delta_{H\text{-}6} - \delta_{H\text{-}6'}) = -0.02$, indicates that the H-6 and/or H-6′ protons in $\mathbf{1}^+$ interact with solvent D_2O. The structure of $\mathbf{1}^+$ in water, however, remains unexplained (vide infra).

For all complexes, the four methyl groups of the equatorial and axial dmso ligands are not equivalent. The conformations of the dmso ligands are restricted, even in the solutions. The two downfield methyl signals were assigned to the equatorial dmso ligand and the remaining two upfield methyl signals are assigned to the axial dmso ligand due to ring-current effects of the bpy ligand in the cis-position.[25] The intracation hydrogen bonds of the axial dmso ligand with H-6′ proton of the bpy and Cl^- ligand, which are observed in the crystal structure, should be evident in the solutions. The conformation of the equatorial dmso ligand is restricted by the bpy and Cl^- ligands through the intracation hydrogen bonds. For $\mathbf{1}^+$, the methyl signals of the equatorial dmso ligand are also nonequivalent, indicating that the H-6′ proton of bpy should form a hydrogen bond with the O atom of a dmso ligand. Therefore, the small difference between H-6 and H-6′ $\Delta(\delta_{H\text{-}6} - \delta_{H\text{-}6'})$ may be caused by the interaction of H-6 with solvent D_2O.

For $\mathbf{1}^+$, $\mathbf{3}^+$, and $\mathbf{4}^+$, the difference in the chemical shift of the methyl signals of the axial dmso ligand ($\Delta\delta = 0.52$, 0.78, and 0.65, respectively) is comparable with that of the precursor *cis*(Cl),*cis*(S)-[Ru(bpy)Cl_2(dmso-*S*)$_2$] ($\Delta\delta = 0.70$), that is the conformation of the axial dmso ligands is also restricted even in the solvents. Although in the crystal the conformation of the axial dmso ligands is depend on the kind of the sixth axial ligand, in the solution the axial dmso ligands have similar conformation in spite of the kind of the sixth axial ligand and the solvent. Therefore, it is suggested that the intracation hydrogen bond of the axial dmso ligand with the equatorial dmso ligand that are observed in the crystal structures of $\mathbf{2}^+$, $\mathbf{4}^+$, and the precursor should also be evident for all complexes in the solutions. For $\mathbf{2}^+$, the four methyl groups of the axial dmso ligands (dmso-*S* and -*O*) are not equivalent. The conformation of axial dmso-*S* ligand may be similar to $\mathbf{1}^+$, $\mathbf{3}^+$, and $\mathbf{4}^+$. Judging by the similarity of the chemical shift and the difference in the chemical shift of the methyl signals, the downfield signal (δ 3.01) and the signal (δ 2.43, $\Delta\delta = 0.58$) can be assigned to the axial dmso-*S* ligand, and the remaining two signals (δ 2.62 and 2.01) to the axial dmso-*O* ligand.

For the above observations of the ^{1}H NMR spectra of $\mathbf{1}^+$, $\mathbf{2}^+$, $\mathbf{3}^+$, $\mathbf{4}^+$, and the precursor, the intracation hydrogen bonding among a bpy, a Cl^-, and two dmso-*S* ligands which are observed in the X-ray crystal structures of $\mathbf{2}^+$, $\mathbf{4}^+$, and the precursor should also be evident to the all complexes even in the solution, in other words, the monodentate ligands, dmso-*S* and Cl^-, in the [Ru(bpy)Cl(dmso-*S*)$_2$]$^+$ unit of structures in $\mathbf{1}^+$, $\mathbf{2}^+$, $\mathbf{3}^+$, and $\mathbf{4}^+$ may be maintained by the hydrogen bonding to be somewhat inert in comparison with the sixth coordination site. As a result, the monodentate ligand L on the sixth coordination site of *trans*(L,S)-[Ru(bpy)Cl(dmso-*S*)$_2$(L)]$^+$ is labile to selective substitution.

Conclusion

The labile cationic aqua complexes, *trans*(O,S)-[Ru(bpy)Cl(dmso-*S*)$_2$(OH_2)]X (**1·X**, $X^- = PF_6^-$ and OTf^-) have been prepared by the treatment of *cis*(Cl),*cis*(S)-[Ru(bpy)Cl_2(dmso-*S*)$_2$] with Ag^+ in water at room temperature. When **1·X** is dissolved in various solvent, DMSO, MeOH, or MeCN, the OH_2 ligand in $\mathbf{1}^+$ is immediately replaced with a solvent molecule (L) to yield *trans*(L,S)-[Ru(bpy)Cl(dmso-*S*)$_2$(L)]$^+$ (L = dmso-*O*, $\mathbf{2}^+$; L = MeOH, $\mathbf{3}^+$; and L = MeCN, $\mathbf{4}^+$), respectively. Moreover, by the reaction of *cis*(Cl),*cis*(S)-[Ru(bpy)Cl_2(dmso-*S*)$_2$] with Ag(OTf) in DMSO on refluxing, **2·(OTf)** is also obtained.

The crystal structures of *trans*(L,S)-[Ru(bpy)Cl(dmso-*S*)$_2$(L)]PF_6 (**1·PF_6·H_2O**, **2·PF_6**, **3·PF_6**, and **4·PF_6·MeCN**) revealed that the structural parameters, except for the sixth axial ligand, were essentially the same, and the four ligands, the bpy, two dmso-*S*, and the equatorial Cl^- ligands are connected by hydrogen bonding as in the case of *cis*(Cl),*cis*(S)-[Ru(bpy)Cl_2(dmso-*S*)$_2$].[25]

All the OH_2, dmso-*O*, MeOH, or MeCN ligands on the sixth coordination site at the axial position in cationic mono(bpy)ruthenium(II) complexes are labile, so they are interconvertable in solution. The [Ru(bpy)Cl(dmso-*S*)$_2$] unit does not break at room temperature, due to the presence of a hydrogen bonding network among the bpy, two dmso-*S*, and the equatorial Cl^- ligands, even in solutions. This hydrogen-bonding interaction was maintained at room temperature at least for 24 h, although it is broken on heating.

These cationic mono(bpy)ruthenium(II) complexes will be very useful precursors of further ruthenium(II)–bpy complexes.

Supporting Information

The ^{1}H NMR spectrum of **2·PF_6** in DMSO-d_6 (Figure S1), ^{1}H NMR spectrum of **3·PF_6** in CD_3OD (Figure S2), ^{1}H NMR spectrum of **4·PF_6·MeCN** in CD_3CN (Figure S3), ^{1}H NMR spectra of **1·PF_6·H_2O** in D_2O after t h of heating at 323 K ($t = 0$ and 3 h) (Figure S4), ^{1}H NMR spectra of **3·PF_6** in CD_3OD after t h of heating at 323 K ($t = 0$ and 3 h) (Figure S5), ^{1}H NMR spectra of **4·PF_6·MeCN** in CD_3CN after t h of heating at 323 K ($t = 0$, 3, and 24 h) (Figure S6), intracation nonbonding contacts for the crystal structures of $\mathbf{1}^+$ in **1·PF_6·H_2O**, $\mathbf{2}^+$ in **2·PF_6**, $\mathbf{3}^+$ in **3·PF_6**, and $\mathbf{4}^+$ in **4·PF_6·MeCN** (Figures S7, S8, S9, and S10, respectively), and intercation hydrogen bonding in crystal structure of **1·PF_6·H_2O** and **3·PF_6** (Figures S11 and S12, respectively) are in PDF format. This material is available free of charge on the web at http://www.csj.jp/journals/bcsj/.

References

1 A. Juris, V. Balzani, F. Barigelletti, S. Campagna, P. Belser, A. von Zelewsky, *Coord. Chem. Rev.* **1988**, *84*, 85.

2 V. Balzani, A. Juris, M. Venturi, S. Campagna, S. Serroni, *Chem. Rev.* **1996**, *96*, 759.

3 F. Barigelletti, L. Flamigni, *Chem. Soc. Rev.* **2000**, *29*, 1.

4 T. J. Meyer, *Pure Appl. Chem.* **1986**, *58*, 1193.

5 Md. K. Nazeeruddin, C. Klein, P. Liska, M. Grätzel, *Coord. Chem. Rev.* **2005**, *249*, 1460.

6 M. Grätzel, *Coord. Chem. Rev.* **1991**, *111*, 167.

7 S. Ito, P. Liska, P. Comte, R. Charvet, P. Péchy, U. Bach, L. Schmidt-Mende, S. M. Zakeeruddin, A. Kay, M. K. Nazeeruddin, M. Grätzel, *Chem. Commun.* **2005**, 4351.

8 C. R. Rice, M. D. Ward, Md. K. Nazeeruddin, M. Grätzel, *New J. Chem.* **2000**, *24*, 651.

9 F. Liu, G. J. Meyer, *Inorg. Chem.* **2005**, *44*, 9305.

10 Y.-Y. Lü, L.-H. Gao, M.-J. Han, K.-Z. Wang, *Eur. J. Inorg. Chem.* **2006**, 430.

11 a) B. Durham, S. R. Wilson, D. J. Hodgson, T. J. Meyer, *J. Am. Chem. Soc.* **1980**, *102*, 600. b) S. W. Gersten, G. J. Samuels, T. J. Meyer, *J. Am. Chem. Soc.* **1982**, *104*, 4029. c) J. A. Gilbert, D. S. Eggleston, W. R. Murphy, Jr., D. A. Geselowitz, S. W. Gersten, D. J. Hodgson, T. J. Meyer, *J. Am. Chem. Soc.* **1985**, *107*, 3855. d) S. Doppelt, T. J. Meyer, *Inorg. Chem.* **1987**, *26*, 2027. e) J. C. Dobson, T. J. Meyer, *Inorg. Chem.* **1988**, *27*, 3283. f) S. J. Raven, T. J. Meyer, *Inorg. Chem.* **1988**, *27*, 4478. g) A. Dovletoglou, S. A. Adeyemi, T. J. Meyer, *Inorg. Chem.* **1996**, *35*, 4120. h) J. R. Schoonover, J. F. Ni, L. Roecker, P. S. White, T. J. Meyer, *Inorg. Chem.* **1996**, *35*, 5885. i) C. W. Chronister, R. A. Binstead, J. Ni, T. J. Meyer, *Inorg. Chem.* **1997**, *36*, 3814. j) R. A. Binstead, C. W. Chronister, J. Ni, C. M. Hartshorn, T. J. Meyer, *J. Am. Chem. Soc.* **2000**, *122*, 8464. k) J. J. Concepcion, J. W. Jurss, J. L. Templeton, T. J. Meyer, *J. Am. Chem. Soc.* **2008**, *130*, 16462.

12 R. A. Leising, J. S. Ohman, K. J. Takeuchi, *Inorg. Chem.* **1988**, *27*, 3804.

13 E. Masllorens, M. Rodríguez, I. Romero, A. Roglans, T.

Parella, J. Benet-Buchholz, M. Poyatos, A. Llobet, *J. Am. Chem. Soc.* **2006**, *128*, 5306.
14 W. Rüttinger, G. C. Dismukes, *Chem. Rev.* **1997**, *97*, 1.
15 M. Yagi, M. Kaneko, *Chem. Rev.* **2001**, *101*, 21.
16 S. Masaoka, K. Sakai, *Chem. Lett.* **2009**, *38*, 182.
17 M.-K. Tsai, J. Rochford, D. E. Polyansky, T. Wada, K. Tanaka, E. Fujita, J. T. Muckerman, *Inorg. Chem.* **2009**, *48*, 4372.
18 H.-W. Tseng, R. Zong, J. T. Muckerman, R. Thummel, *Inorg. Chem.* **2008**, *47*, 11763.
19 M. G. Sauaia, E. Tfouni, R. H. de A. Santos, M. T. do P. Gambardella, M. P. F. M. D. Lama, L. F. Guimarães, R. S. da Silva, *Inorg. Chem. Commun.* **2003**, *6*, 864.
20 N. Chanda, S. M. Mobin, V. G. Puranik, A. Datta, M. Niemeyer, G. K. Lahiri, *Inorg. Chem.* **2004**, *43*, 1056.
21 J. L. Walsh, B. Durham, *Inorg. Chem.* **1982**, *21*, 329.
22 Y. Takahashi, M. Akita, S. Hikichi, Y. Moro-oka, *Inorg. Chem.* **1998**, *37*, 3186.
23 B. Cebrián-Losantos, E. Reisner, C. R. Kowol, A. Roller, S. Shova, V. B. Arion, B. K. Keppler, *Inorg. Chem.* **2008**, *47*, 6513.
24 E. Alessio, G. Mestroni, G. Nardin, W. M. Attia, M. Calligaris, G. Sava, S. Zorzet, *Inorg. Chem.* **1988**, *27*, 4099.
25 M. Toyama, K. Inoue, S. Iwamatsu, N. Nagao, *Bull. Chem. Soc. Jpn.* **2006**, *79*, 1525.
26 H. E. Gottlieb, V. Kotlyar, A. Nudelman, *J. Org. Chem.* **1997**, *62*, 7512.
27 N. Nagao, M. Mukaida, S. Tachiyashiki, K. Mizumachi, *Bull. Chem. Soc. Jpn.* **1994**, *67*, 1802.
28 *teXsan: Crystal Structure Analysis Package*, Molecular Structure Corporation, **1992**.
29 M. Toyama, R. Suganoya, D. Tsuduura, N. Nagao, *Bull. Chem. Soc. Jpn.* **2007**, *80*, 922.
30 E. Alessio, E. Iengo, S. Geremia, M. Calligaris, *Inorg. Chim. Acta* **2003**, *344*, 183.
31 R. Caspar, C. Cordier, J. B. Waern, C. Guyard-Duhayon, M. Gruselle, P. Le Floch, H. Amouri, *Inorg. Chem.* **2006**, *45*, 4071.
32 Y. Ikeda, T. Yamaguchi, K. Kanao, K. Kimura, S. Kamimura, Y. Mutoh, Y. Tanabe, Y. Ishii, *J. Am. Chem. Soc.* **2008**, *130*, 16856.
33 D. H. Gibson, J. G. Andino, M. S. Mashuta, *Organometallics* **2005**, *24*, 5067.
34 J. Concepción, O. Just, A. M. Leiva, B. Loeb, W. S. Rees, Jr., *Inorg. Chem.* **2002**, *41*, 5937.
35 M. J. Heeg, R. Kroener, E. Deutsch, *Acta Crystallogr., Sect. C* **1985**, *41*, 684.
36 A. W. Cordes, B. Durham, W. T. Pennington, B. Kuntz, L. Allen, *J. Crystallogr. Spectrosc. Res.* **1992**, *22*, 699.
37 S. Bonnet, J.-P. Collin, N. Gruber, J.-P. Sauvage, E. R. Schofield, *Dalton Trans.* **2003**, 4654.
38 W. Lackner, C. M. Standfest-Hauser, K. Mereiter, R. Schmid, K. Kirchner, *Inorg. Chim. Acta* **2004**, *357*, 2721.
39 G. J. Leigh, J. R. Sanders, P. B. Hitchcock, J. S. Fernandes, M. Togrou, *Inorg. Chim. Acta* **2002**, *330*, 197.